

## FEATURE ARTICLE

**Metal Ion Solvation in the Gas Phase: The Quest for Higher Oxidation States****A. J. Stace***School of Chemistry, Physics, and Environmental Science, University of Sussex,  
Falmer, Brighton BN1 9QJ, U.K.**Received: March 13, 2002; In Final Form: June 10, 2002*

The gas-phase study of small metal ion–molecule complexes offers one of the few opportunities in which cluster science and condensed phase behavior can relate at a quantitative level. Until recently, however, there remained a fundamental barrier inhibiting further progress in gas-phase experimentation on metal-ion solvation. The majority of metal ions of chemical and biochemical interest in the condensed phase carry a formal charge greater than +1: a situation which contrasts markedly with the observation that most experiments on gas-phase metal ion–molecule complexes have concentrated on singly charged species. However, during the past five years significant progress has been made to redress this imbalance, with the development of new techniques for generating multiply charged metal–ligand complexes in the gas phase. Despite considerable technical difficulties, two quite separate methods (electrospray and pick-up) have been shown to be capable of producing a wide range of doubly and some triply charged metal–ligand cations and, in the case of electrospray, multiply charged anions as well. This review examines some of the challenges these new experiments have presented and how our view of quite basic processes, such as hydrolysis, may be altered as a result of investigations in the gas phase.

**Introduction**

The most frequently quoted cliché associated with the study of clusters, concerns the possibility that they may “bridge the gap” between single atoms or molecules and the condensed phase.<sup>1</sup> In reality, there are few opportunities to realize this objective because the length scale over which many physical properties operate can far exceed the equivalent size of cluster that can be manipulated and studied in a systematic fashion. A prime example is melting: the very elegant experiments of Buffat and Borel<sup>2</sup> show that many millions of atoms are required before the melting point of a cluster even begins to approach that of the bulk solid. However, the techniques required to handle clusters of this size can introduce their own errors into the measurement process: the clusters cannot be studied in isolation, and therefore, questions arise as to how the support medium might influence the end result. Likewise, measurements on the electronic properties of metallic clusters have made

considerable progress toward spanning the gap between the electron orbitals of the isolated atom and the conduction bands of the bulk solid.<sup>3</sup> However, there still remains a gulf between, for example, the bulk work function and ionization energies measured for metallic clusters in the gas phase; again, it is a question of the size of species that can be interrogated in isolation. Table 1 summarizes some examples of physical properties that have been investigated through experiments with clusters. In some respects, the realization of bulk behavior in clusters is probably not the most important goal: many aspects of nanotechnology rest on the identification and characterization of any unique properties finite-sized particles may possess.

One of the few realistic opportunities for identifying macroscopic behavior in a microscopic system lies in the study of ion solvation in the gas phase. The number of solvent molecules contained within the Debye length associated with the ionic atmosphere of a dilute salt solution will be far fewer than is required, for example, to match the melting temperature or the

**TABLE 1: Summary of Measured Physical Properties of Clusters That Have Been Equated with Bulk Behavior**

bulk property	cluster measurement	size of cluster
work function (conduction band development)	ionization energy/ electron affinity <sup>3</sup>	~200 atoms
melting	heating of deposited clusters <sup>2</sup>	> 1 000 000 atoms
structure (regular icosahedra)	mass spectrometry (magic numbers) <sup>4</sup>	~13 atoms
structure (bulk, fcc, hcp, etc.)	electron diffraction <sup>5</sup>	~2000 atoms
ion solvation	gas-phase thermochemistry <sup>6,7</sup>	~10 molecules

**TABLE 2: Comparison between Hydration Enthalpies and a Summation of Individual Reaction Enthalpies for the Attachment of up to Six Water Molecules in the Gas Phase to Each of the Ions Listed Below<sup>8</sup>**

cation	Li <sup>+</sup>	Na <sup>+</sup>	K <sup>+</sup>
$\sum \Delta H_{n,n+1}^a$	-515	-405	-333
$\Delta H_b^b$	-520	-405	-314
anion	F <sup>-</sup>	Cl <sup>-</sup>	Br <sup>-</sup>
$\sum \Delta H_{n,n+1}^a$	-389	-285	-286
$\Delta H_b^b$	-506	-378	-348

<sup>a</sup> Summation of gas-phase enthalpies. <sup>b</sup> Hydration enthalpies based on a value of -1090.8 kJ mol<sup>-1</sup> for the proton.<sup>5</sup>

lattice periodicity of a bulk solid. Table 2 shows comparisons between enthalpy changes associated with gas-phase ions going into bulk water ( $\Delta H_b$ ) and a summation of the first six enthalpy changes associated with the gas-phase reaction:<sup>8</sup>



As can be seen, results for the cations come close to reproducing the bulk hydration enthalpy, and it might be concluded that the presence of six primary shell water molecules is sufficient to reproduce the essential thermodynamics of the solvation process.

Agreement between the two sets of data for the anions is not as good; this may possibly be due to the cluster data representing measurements on an anion that remains on the surface (for example, I<sup>-</sup>).<sup>10</sup> Alternatively, the bulk data could reflect the presence of an excess electron that is partially delocalized away from the anion into a solvent, which itself has a significant electron affinity. For both cations and anions, a more accurate representation of the gas-phase-condensed-phase relationship also requires some knowledge of the stepwise binding energy of a neutral water cluster.<sup>11</sup>

However, even for isolated ions, the discrete picture of solvation or coordination or both offered by gas-phase experiments may have some merit in a quite unexpected area. The local environment experienced by metal ions in biological systems frequently includes two or three water molecules. Prompted by a Lewis acid-base relationship with the metal ion, water molecules often produce OH<sup>-</sup>, which then goes on to attack other molecules in close proximity to the metal. An example of such behavior is Zn<sup>2+</sup> in carbonic anhydrase in which the resultant OH<sup>-</sup> attacks CO<sub>2</sub>.<sup>12</sup> The coordination of these molecules, probably under conditions of dielectric saturation, is more likely to resemble the discrete molecular arrangement determined from cluster studies than the time-averaged picture appropriate for ions in solution at a particular pH.

Despite the wealth of thermodynamic information, almost all gas-phase measurements of the free energy of solvation,  $\Delta G^0$  (and by implication,  $\Delta H^0$  and  $\Delta S^0$ ) have been restricted to singly

**TABLE 3: First and Second Ionization Energies (IE) for a Range of Metals<sup>16</sup>**

metal	1st IE, eV	2nd IE, eV <sup>a</sup>
Mg	7.72	15.46
Ca	6.11	12.03
Ba	5.21	10.09
Cu	7.73	20.29
Ag	7.58	21.5
Au	9.22	20.5
Mn	7.43	15.64
Mg	7.66	15.53
Pb	7.45	15.52
Ho <sup>b</sup>	6.02	11.8

<sup>a</sup> Corresponds to the step  $M^+ \rightarrow M^{2+} + e^-$ . <sup>b</sup> The third IE for Ho is 23 eV.

**TABLE 4: First IE for a Range of Ligands, Together with Values for Dipole Moment ( $\mu$ ) and Polarizability ( $\alpha$ )<sup>a</sup>**

ligand	IE, eV	$\mu$ , D	$\alpha$ , Å <sup>3</sup>
H <sub>2</sub> O	<b>12.62</b>	1.85	1.45
CH <sub>3</sub> CN	<b>12.19</b>	3.92	4.40
CO <sub>2</sub>	<b>13.77</b>	0.0	2.91
C <sub>5</sub> H <sub>5</sub> N	9.25	2.21	<b>9.18</b>
tetrahydrofuran	9.2	1.75	~ <b>9</b>
CH <sub>3</sub> OH	10.85	1.70	3.30
acetone	9.7	2.88	6.4

<sup>a</sup> Values shown in bold are considered to be significant in influencing the stability of a particular complex.<sup>12</sup>

charged ions.<sup>6,7</sup> For the case of alkali metal ions, for example, Na<sup>+</sup>, K<sup>+</sup>, etc., this is the natural oxidation state, but for a very significant number of metals in the periodic table, the +1 state in the condensed phase is nonexistent.<sup>13</sup> Thus, gas-phase experiments involving Mg<sup>+</sup> and Ca<sup>+</sup> may add to our knowledge of ion-molecule interactions, but they will not contribute to our understanding of the behavior of these metal ions in solution. It is interesting to note that gas-phase experiments on Mg<sup>+</sup>(H<sub>2</sub>O)<sub>n</sub> complexes are strongly perturbed by a reaction that leads to the appearance of Mg<sup>+</sup>OH(H<sub>2</sub>O)<sub>m</sub>, where  $m < n$ .<sup>14,15</sup> Because a more realistic description of Mg<sup>+</sup>OH would be Mg<sup>2+</sup>-OH<sup>-</sup>, part of the driving force for this hydrolysis reaction is the desire for magnesium to revert to the stable Mg(II) state. A second contribution to the energetics of this reaction is the presence of a stronger ion-induced dipole interaction between the solvent molecules and Mg<sup>2+</sup> as opposed to Mg<sup>+</sup>.

Clearly, there are very compelling reasons for developing new experiments that can probe the gas-phase behavior of metal ions in oxidation states that are more characteristic of those found in chemistry and biochemistry, for example, Ni(II), Cu(II), Cr(III), etc.<sup>12,13</sup> However, there is one very significant hurdle, which prevents this line of research from being just a natural extension of the techniques that have served the cause of singly charged ions so well. To help understand the problem, Tables 3 and 4 summarize data on those physical properties of metals and ligands (or solvent molecules) that play a role in the interaction between a metal ion, M<sup>n+</sup> and a potential ligand, L. From the list of ionization energies, it can be seen that metal-centered, singly charged complexes are stable because the metals all have values that are significantly lower than those of the ligating molecules. In contrast, the circumstances regarding doubly charged metal ions are dramatically different. In some instances, the difference between the second ionization energy of a metal and the first ionization energy of a molecule is as high as 12 eV. Thus, a single encounter between, for example, Ni<sup>2+</sup> and H<sub>2</sub>O would lead to immediate electron transfer.

Within the context of possible chemical reactivity (including electron transfer), the outcome of a single collision between a

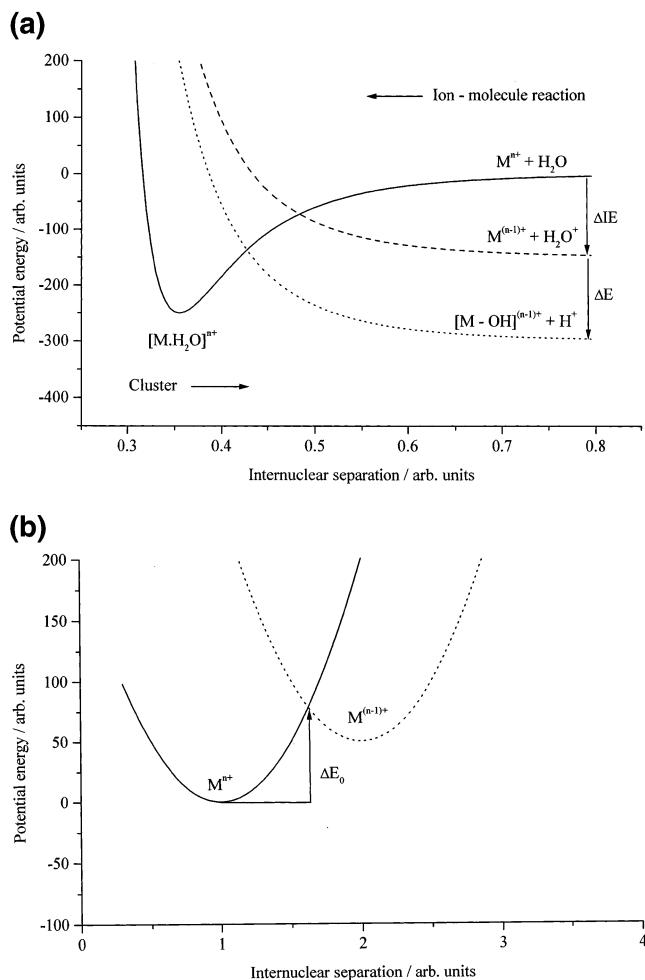


**Figure 1.** Schematic representation of (a) some of the potential energy curves that may exist between a multiply charged metal ion,  $M^{n+}$ , a water molecule, and their electron-transfer products.  $\Delta IE$  is the difference in ionization energy between  $M^{(n-1)+}$  and  $H_2O$ , and  $\Delta H$  represents the exothermicity of the hydrolysis reaction. Panel b shows a schematic representation of the potential energy curves of two metal ions,  $M^{n+}$  and  $M^{(n-1)+}$ , with respect to an arbitrary coordinate separating the ions from a solvent in the condensed phase.  $\Delta E_0$  represents an energy barrier that has to be surmounted for a change in oxidation state to occur.

doubly charged metal ion and a molecule was first analyzed by Tonkyn and Weisshaar.<sup>17</sup> Figure 1a summarizes that analysis in terms of the types of reactions that we might expect to observe in the systems of interest here. A typical molecule ( $H_2O$ ) and a metal ion ( $M^{n+}$ ) are attracted by strong ion–dipole and ion-induced dipole interactions. However, also associated with the potential energy curves are avoided crossings that move the reactants on to repulsive Coulomb potential curves, which have electron-transfer products as their asymptotes.<sup>17</sup> Two separate electron-transfer curves are shown, and the relevance of these to the solvation of  $M^{n+}$  will be discussed later.

As described by Figure 1a, it is the nature of  $M^{n+} + L$  encounters that prevents doubly charged complexes from being “grown” in the gas phase via the route suggested through eq 1. However, this set of circumstances does not necessarily mean that an  $M^{n+}-L$  complex is unstable. In the absence of any internal excitation, such a complex would occupy a position close to the bottom of the attractive potential energy well, and whether this site is stable will depend on the location of the avoided crossing(s).<sup>18–20</sup> If the latter is shifted away from the equilibrium position, then the complex could occupy either a stable or a metastable state. Ions, such as  $[M \cdot H_2O]^{2+}$ , appear

to occupy a stable state with respect to the electron-transfer asymptote,<sup>21</sup> whereas  $[Cu \cdot H_2O]^{2+}$  and  $[Cu \cdot Ar]^{2+}$  are metastable.<sup>22</sup> What is evident from Figure 1a is that the appearance of a stable or metastable state will rely on preparing the complex or its precursor as close to the equilibrium geometry as possible (experimental techniques to achieve this condition are discussed later).

A nice example that illustrates the difficulties experienced when trying to “grow” doubly charged complexes comes from early experiments by Spears et al.<sup>23</sup> These authors studied collisions between alkaline earth metal dications and water and found that  $Mg^{2+}$  underwent immediate electron transfer to give  $MgOH^+$  (cf. Figure 1a).  $Ca^{2+} \cdot H_2O$  could be formed but underwent electron transfer when in collision with a further water molecule, and finally,  $Ba^{2+} \cdot (H_2O)_n$  could be prepared with up to 12 water molecules. It can be seen from the data in Tables 3 and 4 that the results for  $Mg^{2+}$  and  $Ba^{2+}$  can be understood in terms of the difference in ionization energy between the metal atom and a water molecule. The result for  $Ca^{2+}$  is more difficult to understand but could be interpreted in terms of the barrier to electron-transfer being influenced by the binding energy of the second water molecule (see below).

Clearly, the circumstances for  $M^{n+}$  in solution are quite different from those experienced in the gas phase with just a few water molecules. Figure 1b illustrates one possible relationship between two oxidation states,  $M^{n+}$  and  $M^{(n-1)+}$ .<sup>24</sup> Ions in the  $n+$  and  $(n-1)+$  states occupy deep potential wells defined by their respective solvation energies, and the movement between states requires an input of energy, possibly in the form of an electromagnetic force (emf) or a photon.<sup>25,26</sup> In the gas phase, it has been shown that the energy barrier between states,  $\Delta E_0$ , can be overcome through collisional or photoexcitation.<sup>27,28</sup> The arrangement depicted in Figure 1b further distinguishes multiply charged from singly charged ions: in solution, stability of the former relies on an implicit relationship between the ion and the solvent (or coordinating ligands), and a change in solvent or ligand geometry or both can shift an equilibrium in the direction of a particular oxidation state. For example, the redox potential of the Cu(I)/Cu(II) couple can be influenced by selecting ligands that force the ion to adopt tetrahedral geometry.<sup>25</sup> In the case of transition metal ions, these stability relationships also extend into the realm of ligand field theory, whereby ligand field stabilization energy can contribute to the solvation energy of an ion.<sup>13</sup>

The successful observation of multiply charged metal–ligand complexes in the gas-phase relies, in part, on acknowledging how those same ions behave in the bulk. Thus, the cation  $[Ag \cdot (\text{pyridine})_4]^{2+}$  in association with  $S_2O_8^{2-}$  as a counterion is a stable condensed-phase compound,<sup>13</sup> and Ag(II)/pyridine complexes are comparatively easy to prepare in the gas phase.<sup>29</sup> However,  $Ag^{2+}$  rapidly oxidizes water at pH 7,<sup>13</sup> and complexes of the form  $[Ag \cdot (H_2O)_n]^{2+}$  cannot be prepared in the gas phase.<sup>29,30</sup> As discussed below, the absence of a permanent hydrogen ion concentration (pH) in a water cluster has an interesting influence on the behavior of certain metal ions.

### Techniques for Preparing Multiply Charged Metal–Ligand Complexes in the Gas Phase

There are two quite separate, but very effective methods for generating multiply charged metal–ligand or –solvent complexes in the gas phase. The first and most widely used is electrospray,<sup>31,32</sup> in which the ions of interest are prepared in the liquid phase prior to entry into the gas phase under vacuum. Part of the rationale behind using electrospray for such experi-

ments was the desire to sample ionic solutions “in situ”.<sup>33</sup> Kebarle and co-workers<sup>31,32</sup> were the first to use this approach in a series of systematic studies of doubly and triply charged complexes. More recently, this group has used electrospray in combination with collision-induced dissociation to measure metal ion–ligand binding energies.<sup>34</sup> In related experiments, Williams and co-workers<sup>35–37</sup> have combined electrospray with Fourier transform ion cyclotron resonance (FTICR) ion storage to determine ion binding energies for a range of doubly charged complexes containing alkaline earth metals. Several groups have also used electrospray for the purposes of studying the spectroscopic properties of metal ion complexes. Posey et al.<sup>38,39</sup> have successfully used the technique to study electron-transfer spectra in Fe(II)-based systems, and very recently, Metz and co-workers<sup>40,41</sup> have reported results on the electronic spectra of Ni<sup>2+</sup> and Co<sup>2+</sup> complexes with water, which were generated using electrospray. Electrospray appears to be particularly effective at generating metallic complexes of biochemical interest, of which ligands may have vapor pressures that are too low for use in the method discussed below.<sup>42</sup>

An alternative method for generating stable ion complexes that has been developed within the group at Sussex uses a “pick-up” technique.<sup>27,29,30,43,44</sup> Neutral clusters of the desired combination are prepared first by passing solvent/argon clusters over an oven that is generating  $\sim 10^{-3}$  mbar of metal vapor. The resultant metal/solvent clusters are then ionized by high-energy ( $\sim 100$  eV) electron impact. The end result is a multiply charged metal ion encapsulated in a stable solvent environment, which can be created from a very broad range of materials; the only requirement is that the solvent or ligand has sufficient vapor pressure to generate gas-phase clusters. Candidate solvents include many of the traditional inorganic ligands, such as pyridine,<sup>29,44,45</sup> tetrahydrofuran,<sup>46</sup> and acetonitrile,<sup>29,30,44</sup> and several new ligands that have not been utilized previously but still have the ability to stabilize a multiply charged metal ion. CO<sub>2</sub> is an excellent example of the latter and is effective primarily because of its high ionization energy.<sup>30,43</sup> Using the “pick-up” technique, we have generated multiply charged complexes from a wide range of metals, including the transition elements Cu,<sup>27,44,47</sup> Ag,<sup>29</sup> Au,<sup>30,45</sup> Mn,<sup>48,49</sup> and Cr<sup>50</sup> and the alkaline earth metals Mg<sup>43,46,51</sup> and Sr.<sup>52</sup> The method has also been used to produce complexes with metals in oxidation states that are difficult to observe in the bulk phase, for example, Au(II) in the form of [Au(pyridine)<sub>4</sub>]<sup>2+</sup>.<sup>45</sup> With the use of commercial Knudsen cells, there are fewer than 10 metals in the periodic table that would not be accessible to study using the pick-up technique.

Figure 2 shows a typical mass spectrum recorded using the pick-up technique in association with a high-resolution, double-focusing mass spectrometer (VG-ZAB E). Because the method of preparation relies on first generating solvent and solvent/argon clusters, subsequent mass spectra reflect the presence of these “starting materials”. However, the use of high-resolution mass spectrometry helps with the identification and isolation of the ions of interest. Possibly the single most significant advantage of the pick-up technique when compared with electrospray is the very diverse range of ligands that can be studied. In some instances, only the pick-up method has thus far provided access to certain complexes that have played a pivotal role in solution-phase transition metal chemistry, for example, [Cu(NH<sub>3</sub>)<sub>n</sub>]<sup>2+</sup>.<sup>44,53</sup>

Associated with the apparatus developed at Sussex are two techniques for investigating the properties of multiply charged metal–ligand complexes. Collisional activation has been used

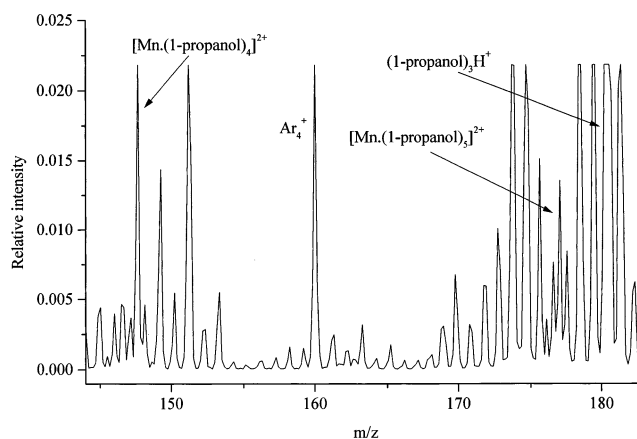


**Figure 2.** Sample mass spectrum recorded following the electron impact ionization of complexes formed between manganese and 1-propanol. Several doubly charged ions are identified, as is Ar<sub>4</sub><sup>+</sup>, which is used as a mass marker.

**TABLE 5: Data Derived from Intensity Distributions Recorded for a Range of [M·L<sub>n</sub>]<sup>2+</sup> Complexes<sup>a</sup>**

ligand	metal					
	copper		silver		magnesium	
	<i>n</i> <sub>min</sub>	<i>I</i> <sub>max</sub>	<i>n</i> <sub>min</sub>	<i>I</i> <sub>max</sub>	<i>n</i> <sub>min</sub>	<i>I</i> <sub>max</sub>
H <sub>2</sub> O	3	8			2	4–6
CH <sub>3</sub> OH	3	8			2	5–10
pyridine	2	4	2	4	2	4
CH <sub>3</sub> CN	2	4	2	4	1	4
CO <sub>2</sub>	1	4	2	4	2	4
tetrahydrofuran	2	4	4	5	2	4
acetone	3	4	4	5	3	4

<sup>a</sup> *n*<sub>min</sub> is the minimum value of *n* for which a stable complex could be observed, and *I*<sub>max</sub> is the value of *n* with the highest intensity.<sup>29,43,44</sup>

to promote a range of chemical reactions, including the loss of neutral ligands and electron transfer in the form of both reduction and oxidation of the central metal cation. Laser excitation with UV and visible radiation has been used to study ligand-to-metal charge (electron) transfer (LMCT) and to promote ligand field transitions in the form of ligand–d and d–d electron excitation.<sup>54,55</sup>

### Stable [ML<sub>m</sub>]<sup>n+</sup> Combinations—Electronic and Structural Consequences

There are two qualitative, but at the same time significant, measurements that can be made from a simple mass spectrum of multiply charged complexes. It could be anticipated from both Figure 1a and the data presented in Tables 3 and 4, that there should exist a minimum size, *n*<sub>min</sub>, below which the combination [M·L<sub>m</sub>]<sup>n+</sup>, *m* < *n*<sub>min</sub>, is unstable with respect to electron transfer. There are two ways that an experimental value for *n*<sub>min</sub> can be recorded: (i) by noting the absence of a particular ion from a mass spectrum or (ii) by taking a stable complex [M·L<sub>m</sub>]<sup>n+</sup> for *m* > *n*<sub>min</sub> and observing the nature of the products following photo- or collisional-activation. Table 5 lists a range of values for *n*<sub>min</sub> that have been recorded from experiments in which the pick-up technique has been used to prepare the ions.<sup>43,44</sup> Some of these measurements have been the subject of a recent controversy, which took the form of a discussion on the possible stability of the dimer ions [Cu·H<sub>2</sub>O]<sup>2+</sup> and [Cu·NH<sub>3</sub>]<sup>2+</sup>,<sup>56,57</sup> theory suggested that these ions should be stable,<sup>56</sup> but their presence could not be detected in either mass spectra or ion fragmentation patterns recorded from pick-up experiments.<sup>57</sup>

Experimental evidence regarding the stability of both  $[\text{Cu}\cdot\text{H}_2\text{O}]^{2+}$  and  $[\text{Cu}\cdot\text{NH}_3]^{2+}$  has recently been provided by Schroder et al.<sup>58</sup> from charge-stripping experiments, and additional confirmation of the stability of  $[\text{Cu}\cdot\text{H}_2\text{O}]^{2+}$  has come from electrospray experiments by Stone and Vukomanovic.<sup>59</sup> In addition, Shvartsburg and Siu have recently shown that it is possible to generate  $[\text{M}\cdot\text{H}_2\text{O}]^{2+}$  dimer ions for a wide range of first-row transition metals using electrospray.<sup>60</sup> Extending this discussion to other systems, it can be seen from Table 5 that very small metal/ligand combinations are not routinely seen in pick-up experiments. The current situation can probably be summarized as follows: provided there are no curve crossings close to the equilibrium geometry (Figure 1a), theory can probably locate metastable bound states for complexes, such as  $[\text{Cu}\cdot\text{H}_2\text{O}]^{2+}$ , irrespective of how shallow the well is (zero-point energy included); however, these metastable states may not always be accessible using experimental techniques such as the pick-up method.

What may ultimately prove to be a more significant measurement is one that demonstrates whether a metal ion can form a stable gas-phase complex with a particular type of ligand irrespective of the number involved. For example, both Ag(II) and Au(II) will not form stable complexes with either water or a wide range of alcohols under any conditions.<sup>29,30</sup> Likewise, Sn(II),<sup>33</sup> Pb(II),<sup>61,62</sup> and Hg(II)<sup>33</sup> will not form stable complexes in the gas phase with water but instead undergo a hydrolysis reaction to form  $\text{M}^+\text{OH}(\text{H}_2\text{O})_n$ ; similar behavior is seen on the part of triply charged metal ions, such as those from the lanthanide series La(III),<sup>63</sup> Sm(III),<sup>63</sup> and Ho(III).<sup>64</sup> The behavior of multiply charged ions in the presence of hydrogen-bonded solvents, such as water and methanol, together with the significance of the hydrolysis reaction in the gas phase, is discussed below. However, it is very probable that the general topic of stability within  $[\text{M}\cdot\text{L}_n]^{n+}$  complexes will stimulate considerable debate over the next few years.

A second measurement that can be made from a mass spectrum is  $I_{\text{max}}$ , the size of  $[\text{M}\cdot\text{L}_m]^{n+}$  combination that has the maximum intensity. The question then arises as to whether  $I_{\text{max}}$  can be equated with the formation of a particularly stable ion. Addressing the situation with regard to the pick-up process first, the circumstances regarding the final observation of an ion are as follows. Electron impact ionization in conjunction with the formation of highly charged ions is a comparatively violent process, which leaves ions with a high internal energy, possibly in the form of electronic as well as vibrational excitation. However, ions reaching the detector of a mass spectrometer are approximately  $10^{-4}$  s old, and as such they will have had an opportunity to undergo radiative decay or to shed molecules or both to reduce their internal energy content. Because there are no opportunities for ions to “grow” through association, this is a strictly nonequilibrium system whereby all ions undergo some form of decay. What distinguishes one particular ion from its neighbors is the rate of decay over the period of observation ( $\sim 10^{-4}$  s)—ions with **relatively** high internal energies or **relatively** low binding energies or both will have high rates of decay; in contrast, stable ions will decay less rapidly. This comparatively simple concept can be used to explain the evolution of “magic numbers” in the mass spectra of molecular and rare gas cluster ions.<sup>65</sup> Lethbridge and Stace have modeled the effects on a mass spectrum of a systematic variation in binding energy between different-sized rare gas cluster ions,<sup>66</sup> and changes in the relative intensities of neighboring ions as a result of variations in observation time have also been equated with the evolution of stable structures.<sup>67</sup> In conclusion, as a

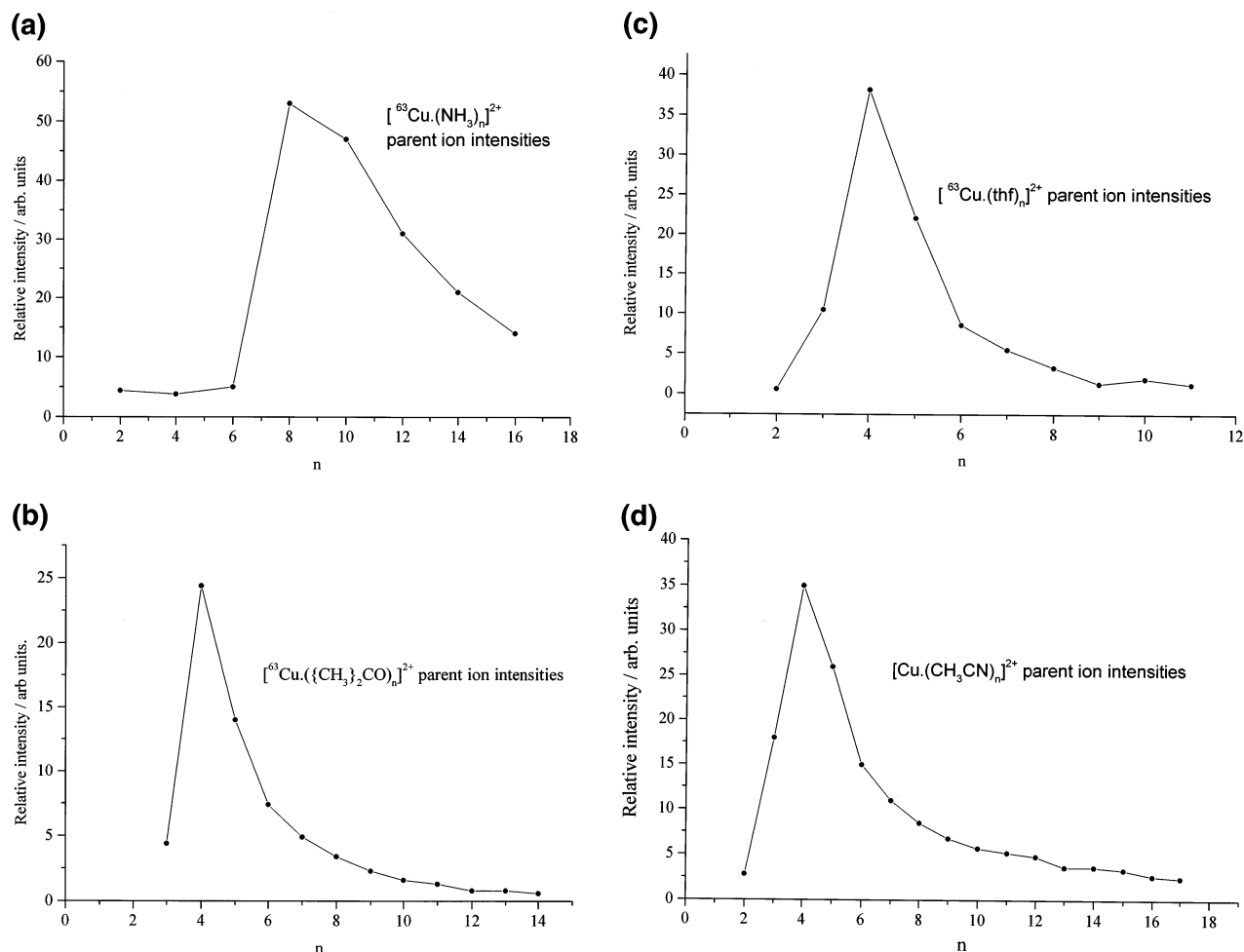
function of time stable ions gain in intensity at the expense of less-stable neighbors. However, it should be emphasized that the differences are relative; hence, the approach works equally well for transition metal complexes as it does for rare gas cluster ions, despite orders of magnitude differences in binding energy.

Figure 3 gives examples of intensity distributions recorded for several Cu(II)/ligand combinations, and Table 5 gives values of  $I_{\text{max}}$  for a series of different metal/ligand complexes. In addition to the factors identified above, the intensities of multiply charged ions are subject to one further constraint, which is that small ions tend to be unstable with respect to electron transfer. Therefore, there is a natural tendency for each distribution to shift toward smaller sizes through unimolecular decay, but once below some critical size,  $n_{\text{crit}} \geq n_{\text{min}}$ , the ions can be further depleted through Coulomb explosion. Given that these two conditions serve to deplete intensity from opposite ends of a distribution (electron-transfer rates are at their highest for very small complexes), it could be just fortuitous that most distributions peak at  $I_{\text{max}} = 4$ . However, many condensed-phase compounds for which an analogous gas-phase complex can be identified do have coordination numbers of four, for example,  $[\text{Ag}\cdot(\text{pyridine})_4]^{2+}$ ,  $[\text{Cu}\cdot(\text{pyridine})_4]^{2+}$ , and  $[\text{Mg}(\text{thf})_4]^{2+}$ .<sup>13</sup> Other factors, such as Jahn–Teller distortion, may be responsible for a preferential weakening of axial bonds in Ag(II) and Cu(II)  $d^9$  metal ions, in which case measurements in the gas phase could be very sensitive to the kinetic consequences of that process (see below for further examples of where Jahn–Teller distortion is thought to have an influence on behavior).

However, it has long been recognized in the study of clusters ions that to underpin any conclusions regarding preferential stability or the appearance of “magic numbers”, it is necessary to examine the fragmentation patterns of the ions concerned.<sup>65</sup> Quite a nice illustration of the type of response expected of excited ions comes from a recent study of the fragmentation patterns of  $[\text{Cu}\cdot(\text{pyridine})_n]^{2+}$  complexes excited at UV wavelengths ( $\pi^* \leftarrow \pi$  transition on pyridine at 280 nm or 4.42 eV).<sup>54</sup> The results are shown in Figure 4, in which it can be seen that for  $n \leq 4$  the fragments consist of a mixture of electron-transfer products and a single neutral molecule. However, for  $n > 4$  there is a very consistent pattern, which results in 90% of all ions fragmenting down to the stable unit  $[\text{Cu}\cdot(\text{pyridine})_4]^{2+}$ . What is particularly satisfying about this result is that even the  $n = 5$  complex preferentially decays to  $[\text{Cu}\cdot(\text{pyridine})_4]^{2+}$ ; because the  $n = 3$  complex is also stable, some fragmentation to that ion might have been anticipated if there were not some form of kinetic barrier associated with  $n = 4$ . Similar results were recorded for  $[\text{Ag}\cdot(\text{pyridine})_n]^{2+}$  complexes.<sup>54</sup> If such behavior is repeated in a typical electron impact experiment, then it is obvious that the consequences will be a significant gain in intensity on the part of stable ions.

Not all complexes exhibit maximum stability at  $n = 4$ ; almost all of the ions formed with benzene have peak intensities at  $I_{\text{max}} = 2$ , which is believed to reflect the formation of sandwich-like structures. Similarly, many of the complexes formed with hydrogen-bonded solvents have values of  $I_{\text{max}} > 4$  (see below), and those prepared with Ho(III) using aprotic ligands mostly yielded  $I_{\text{max}} = 6$ .<sup>64</sup>

Relative ion intensities recorded during a typical pick-up experiment are virtually independent of the initial conditions. Solvent/argon composition, expansion pressure, oven temperature, and electron impact energy can affect absolute intensities but have very little influence over the fluctuations in intensity that are seen across any recorded distribution. This observation is probably a consequence of the rather violent conditions under



**Figure 3.** Distribution of relative intensities recorded for (a)  $[\text{}^{63}\text{Cu}(\text{NH}_3)_n]^{2+}$ , (b)  $[\text{}^{63}\text{Cu}(\{\text{CH}_3\}_2\text{CO})_n]^{2+}$ , (c)  $[\text{}^{63}\text{Cu}(\text{thf})_n]^{2+}$ , and (d)  $[\text{}^{63}\text{Cu}(\text{CH}_3\text{CN})_n]^{2+}$ . Adapted from ref 44.

which the ions are prepared; however, the collision-free environment of the ion source and the remainder of the mass spectrometer means that parameters that influence unimolecular decay, such as the degree of internal excitation and the binding energy, become paramount in determining the shape of the final ion distribution. This situation contrasts markedly with electrospray, in which the relative intensities of ions are very sensitive to the conditions, such as injection energy and location of the injection needle, that prevail in the ion source at the time of preparation.<sup>68,69</sup> The degree of collisional heating, which is determined by the injection energy in an electrospray source, can have the effect of shifting intensity profile maxima either upward or downward.<sup>68</sup> Thus, there are examples in which the results of relative intensity measurements from pick up and electrospray agree, but this is achieved by making adjustments to the operating conditions of the latter technique.<sup>27,68</sup>

### Observations of the Behavior of $\text{M}^{2+}$ and $\text{M}^{3+}$ Ions with Hydrogen-Bonded Solvents and Ligands

It is quite clear from a range of experimental and theoretical studies on multiply charged metal complexes, that behavior in hydrogen-bonded solvents is somewhat different from that seen with either aprotic ligands in the gas phase or most (including H-bonded) ligands in the condensed phase. Although this topic has been the subject of brief review,<sup>70</sup> we shall use this opportunity to summarize some of the more recent ideas and results.

**(i) The Influence of Hydrogen Bonds on the Development of Structure.** Figure 5 summarizes some recent results on

structures calculated for particular combinations of a doubly charged metal ion with small numbers of water molecules.<sup>49,71–73</sup> The three structures shown embrace a range of situations, some of which have been supported by experimental data. The structure shown in Figure 5a was originally proposed by Berc, Zeigler, and co-workers to account for the experimental observation that the gas-phase complex  $[\text{Cu}(\text{H}_2\text{O})_8]^{2+}$ <sup>71</sup> was the most intense ion observed in a study of  $\text{Cu}(\text{II})/\text{water}$  complexes using the pick-up technique.<sup>27</sup> A similar result has recently been reported using electrospray.<sup>68</sup> The structure consists of a square-planar arrangement of water molecules to which a further four molecules are attached via double-acceptor hydrogen bonds. These sites are populated in preference to two of the water molecules occupying axial sites directly on the metal ion, the energy difference being  $\sim 70 \text{ kJ mol}^{-1}$ . Similar experimental results were presented for  $[\text{Cu}(\text{NH}_3)_8]^{2+}$ ,<sup>53</sup> and even though the ammonia molecule can only form one acceptor bond, the extended square-planar, hydrogen-bonded structure was again calculated to be more stable than a primary solvation shell with an octahedral configuration.<sup>71</sup> Applying the ideas discussed above regarding the energetics and kinetics of ion fragmentation, we would conclude that molecules occupying the Jahn–Teller distorted axial sites on  $\text{Cu}(\text{II})$  are less strongly bound than those occupying hydrogen-bonded sites in the secondary solvation shell.

These results do not contradict observations from solution-phase chemistry, which report octahedral  $[\text{Cu}(\text{H}_2\text{O})_6]^{2+}$  and  $[\text{Cu}(\text{NH}_3)_6]^{2+}$  complexes as the primary solvation units.<sup>74</sup> In solution, molecules are free to move in and out of the axial

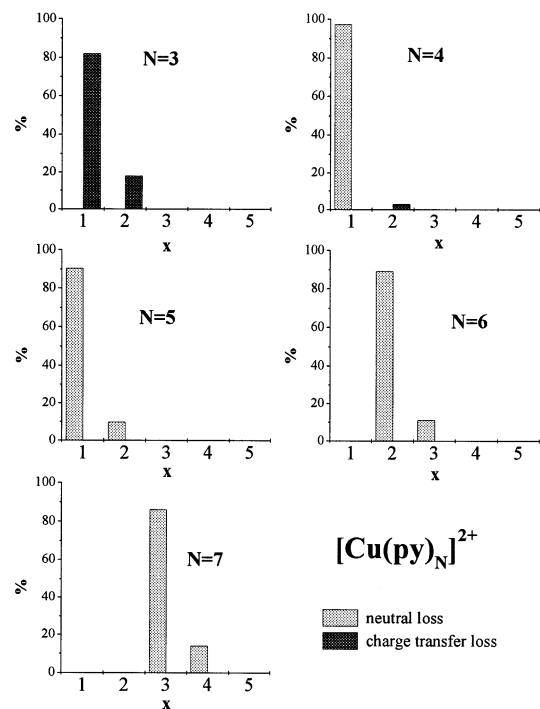


**Figure 4.** Relative intensities of photofragments recorded following the excitation of selected  $[\text{Cu}(\text{py})_n]^{2+}$  complexes at 280 nm. Each plot shows the number of molecules lost,  $x$ , either all in the form of neutral molecules or accompanied by one electron-transfer product. Adapted from refs 50 and 55.

sites, and in Cu(II), these exchange times are particularly rapid; therefore, a time-averaged picture would show a more or less uniform distribution of water molecules. However, such experiments provide no details of the energetics associated with displacing water molecules, and therefore,  $[\text{Cu}(\text{H}_2\text{O})_6]^{2+}$  need not necessarily be the most stable unit. In contrast, the nature of the gas-phase experiment is such that the end result is very sensitive to small differences in relative binding energy.

Figure 5b shows the lowest-energy structure calculated for the complex  $[\text{Mn}(\text{H}_2\text{O})_6]^{2+}$ , in which the molecules occupy a 4 + 2 configuration and the primary solvation shell has tetrahedral symmetry.<sup>49</sup> Similar structures have been calculated for other “closed-shell” ions,<sup>72</sup> such as  $\text{Zn}^{2+}$  and  $\text{Be}^{2+}$ , but for  $\text{Mg}^{2+}$  and  $\text{Ca}^{2+}$  the most stable structures with water have octahedral symmetry.<sup>72</sup> What is interesting about the tetrahedral structure is that, unlike the square-planar arrangement shown in Figure 5a, only two further water molecules can be accommodated in a secondary solvation shell. Any remaining sites are not favorably displaced for the formation of further double hydrogen bonds. Recent experiments have provided confirmation that, in the gas phase,  $[\text{Mn}(\text{H}_2\text{O})_4]^{2+}$  is a stable solvation unit.<sup>49</sup> With the addition of one more water molecule to the 4 + 2 structure, the preferred site involves direct coordination to the metal ion. Thus  $\text{Mn}^{2+}$  in the gas phase could gradually build up a solvation shell that resembles that attributed to the ion in the bulk phase;<sup>74</sup> however, the route leading to such an arrangement is not the most obvious.

Finally, Figure 5c shows the minimum-energy structure calculated for  $[\text{Pb}(\text{H}_2\text{O})_4]^{2+}$  in which the preferred geometry is for a 3 + 1 arrangement of water molecules.<sup>73</sup> The structure is strongly influenced by the presence of an inert  $6s^2$  electron pair on Pb(II), which gains sufficient “p” character to become stereochemically active. The result is that ligand–lone pair repulsion pushes the water molecules into a hemidirectional

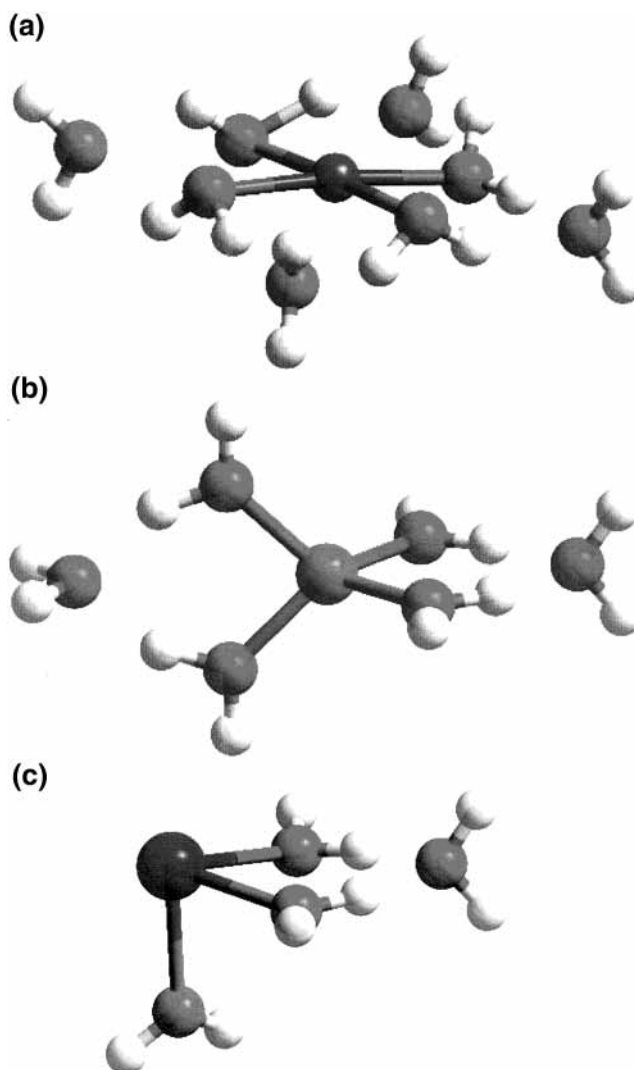
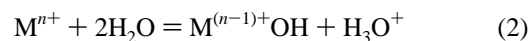


**Figure 5.** Series of structures calculated to be minimum-energy configurations for doubly charged metal ions in association with water: (a)  $[\text{Cu}(\text{H}_2\text{O})_8]^{2+}$  (new calculation<sup>47</sup> based on the structure originally proposed by Bérces et al.<sup>71</sup>); (b)  $[\text{Mn}(\text{H}_2\text{O})_6]^{2+}$ ;<sup>49</sup> (c)  $[\text{Pb}(\text{H}_2\text{O})_4]^{2+}$ .<sup>61</sup>

configuration, which in its lowest energy form can only accommodate three molecules in the primary solvation shell. Additional molecules then occupy sites in the secondary shell.<sup>73</sup> The effect that this arrangement has on the chemistry of Pb(II) is discussed below.

**(ii) The Hydrolysis Reaction—The Chemical Consequence of H-Bond Formation.** One particular aspect of the study of multiply charged metal–ligand complexes that has attracted attention is the gas-phase equivalent of the hydrolysis reaction:



There is also growing evidence of a select group of doubly charged metal ions that will not form stable complexes in the gas phase with water, irrespective of how many molecules are present. Gold(II) and silver(II) have already been mentioned but will not be discussed any further because of the almost complete absence of any condensed-phase data on these ions in water. Other examples that have been identified from both electrospray and pick-up experiments are Sn(II),<sup>33</sup> Hg(II),<sup>33</sup> and Pb(II).<sup>61,62</sup> In all cases, the ions observed have the form  $\text{M}^+-\text{OH}(\text{H}_2\text{O})_n$ , which suggests that if the experiments do generate

**TABLE 6: Data Correlating the Behavior of  $M^{2+}$ – and  $M^{3+}$ –Water Complexes in the Gas Phase with the Properties of Metal Ions in Solution**

$M^{2+}$	$\sim pK_h^a$	stable as gas-phase complex	acid <sup>b</sup>	$q^2/r^c$	$\Delta H_h$ , kJ mol <sup>-1 d</sup>
Be	5–6	yes	h	5.68	2485
Mg	11	yes	h	3.55	1920
Ca	12	yes	h	2.56	1590
Sr	13	yes	h	2.16	1443
Ba	13	yes	h	1.89	1301
Cr	9	yes	yes	3.20	1846
Mn	11	yes	h	3.08	1843
Fe	9	yes	b	3.28	1918
Co	9	yes	b	3.41	2053
Ni	10	yes	b	3.71	2104
Cu	7	yes	b	4.49	2098
Zn	9	yes	b	3.50	2042
Cd	8	yes	s	2.69	1804
Sn	2	no	b	2.75	1550
Hg	3–4	no	s	2.66	1819
Pb	8	no	b	2.15	1478
Ag		no <sup>e</sup>		3.24	
Au		no <sup>e</sup>		2.43	

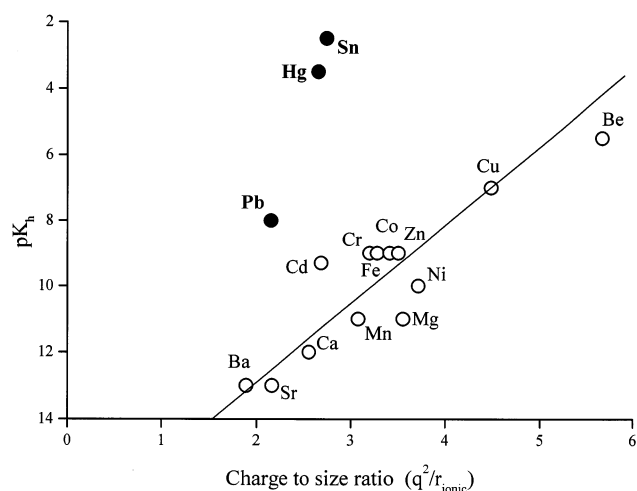
  

$M^{3+}$	$\sim pK_h^a$	stable as gas-phase complex	acid <sup>b</sup>	$q^3/r^f$	$\Delta H_h$ , kJ mol <sup>-1 d</sup>
Ce	9	no	h	4.05	3550
La	7–10	no	h	3.53	3280
Nd	7–9	no	h	3.53	3420
Yb	7–9	no	h	3.94	3740
Ho	5–8	no	h	3.82	3600
Al	5	no	h	7.58	4657
Sc	4–5	no	h	4.71	3958
Sm	4–8	no	h	3.10	3500
Cr	4	no	h	6.71	4560
Fe	2	no	h	6.30	4430
Co	1	no	h	6.71	4651

<sup>a</sup> Defined by equations 3 and 4 and where possible measured at zero ionic strength. Data taken from ref 75. <sup>b</sup> HSAB classification: h = hard; s = soft; b = borderline. Data taken from ref 76. <sup>c</sup> Charge-to-size ratio in units of  $C^2 m^{-1} \times 10^{28}$ . <sup>d</sup> Hydration enthalpy based on a value of  $-1090.8$  kJ mol<sup>-1</sup> for the proton. Data taken from ref 9. <sup>e</sup> Known not to form stable complexes with water in the condensed or gaseous phase. <sup>f</sup> Charge-to-size ratio in units of  $C^3 m^{-1} \times 10^{47}$ .

$[M \cdot (H_2O)_n]^{2+}$  ions, then they immediately undergo hydrolysis (as depicted in Figure 1a). In some respects, it is possible to assume that the metal ion retains a formal charge of +2 by considering  $M^+OH$  to be of the form  $M^{2+}-OH^-$ . In certain circumstances, the hydrolysis reaction can also be promoted in singly charged complexes, for example, those involving alkaline earth metals, for example,  $Mg^+(H_2O)_n$ , in which it is thought that formation and solvation of the polar unit  $Mg^{2+}-OH^-$  is the driving force behind the reaction.<sup>14,15</sup> Because  $Mg^+$  is probably only stable in the gas phase, hydrolysis is one route to achieving the more common oxidation state. Recent experiments have shown the lead ion, Pb(II), to exhibit an interesting pattern of behavior,<sup>61</sup> in that complexes of the form  $[Pb \cdot (ROH)_n]^{2+}$  are unstable when  $R = H, Me,$  and  $Et$  but can be seen in the mass spectrometer when the alcohol ligand is either propanol or butanol. At a qualitative level, this behavior has been attributed to a softening of the base (ROH) to match the acidity of Pb(II). Supporting density functional calculations (DFT) show that the degree of covalent bonding between Pb(II) and ROH increases on going from  $R = H$  to  $R = propyl$ .<sup>61</sup> It is not altogether clear whether, at a molecular level, similar factors might also be responsible for the instability of Sn(II) and Hg(II) in the presence of a finite number of water molecules.

Table 6 summarizes the current situation regarding the observation of stable  $[M \cdot (H_2O)_n]^{2+}$  complexes in the gas phase.



**Figure 6.** Plot of the hydrolysis constant,  $pK_h$ , as a function of the charge-to-size ratio for selected doubly charged metal ions. The position of the line is arbitrary but is designed to link “closed-shell” ions, such as  $Ba^{2+}$  and  $Ca^{2+}$ . These data have been adapted from ref 77.

Also listed is a selection of the physical characteristics of metal ions, some of which have previously been identified with the ease with which the ions undergo hydrolysis reactions in the condensed phase.

The quantities  $K_h$  and  $pK_h$  are defined as

$$K_h = \frac{[M(OH)^{(n-1)+}][H_3O^+]}{[M^{n+}]} \quad (3)$$

$$pK_h = -\log_{10}(K_h) \quad (4)$$

Figure 6 shows experimentally determined values of  $pK_h$  for a wide range of doubly charged metal ions plotted against charge-to-size ratio ( $q^2/r_{ion}$ ) for each of the ions.<sup>77</sup> Where possible, the size of an ion has been taken to be the ionic radius as determined in water as a solvent. The line drawn through the data links “closed-shell” ions, such as  $Ca^{2+}$ , for which the geometry of the primary solvation shell will be determined purely by ligand–ligand repulsion and will not include ligand field contributions. Likewise, the hydrolysis product  $Ca(II)OH^-$  can be expected to retain a strong ionic character.  $pK_h$  could be viewed as a measure of the work done to remove a proton from a metal ion–water complex to infinity.<sup>77</sup> Similarly, the electrostatic term,  $q^2/r_{ion}$ , reflects the contribution that Coulomb repulsion between the two separating charges makes to the energetics of proton release.<sup>77</sup> Thus, the degree of repulsion is negligible for the large  $Ba^{2+}$  ion but makes a very significant contribution to the exothermicity of reaction 2 for  $Be^{2+}$ . Also listed for each of the metal ions in Table 6 are hydration enthalpies ( $\Delta H_h$ ), which also provide a similar correlation with  $pK_h$ ; this is not too unexpected because the factor  $q^2/r_{ion}$  is also a leading term in the Born equation for the free energy of solvation of an ion.<sup>78</sup>

What is evident from Figure 6 is that three metal ions, Sn(II), Pb(II), and Hg(II), stand out from the qualitative trend that unites the remaining cations. Thus, both the condensed-phase data and gas-phase observations suggest that these three ions are more acidic than would be predicted purely from their size. What may link the gaseous and condensed phases is the way in which the metal ion develops a primary solvation shell: in the gas phase, this process appears to be responsible for the complete absence of stable  $[Pb \cdot (H_2O)_n]^{2+}$  complexes,<sup>73</sup> and in the condensed phase, it influences the magnitude of  $pK_h$ . It has been noted that the behavior of Sn(II), Hg(II), and Pb(II) could be



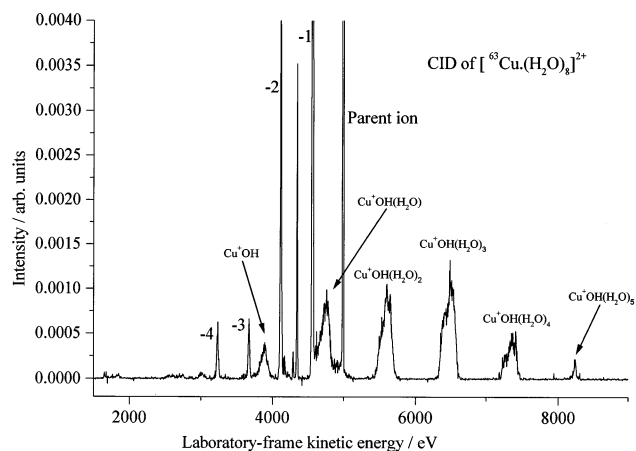


**Figure 7.** Fragmentation pattern recorded for  $[\text{Cu}\cdot(\text{H}_2\text{O})_8]^{2+}$  following collision-induced dissociation (CID) of the size-selected ion. The parent ion has a laboratory-frame kinetic energy of 5 keV, and fragments are identified according to changes in kinetic energy as a result of dissociation. The narrow peaks denoted as  $-k$  correspond to the loss of  $k$  neutral molecules, and the broad peaks arise from electron-transfer processes for which individual charged fragments are labeled separately.

attributed to their “softness”;<sup>79</sup> however, other ions, for example, Cd(II) and Cu(II), which fall into similar HSAB categories, do form stable hydrated complexes both in the condensed phase and with finite numbers of water molecules (see Table 6).

An important distinction between bulk water and a finite collection of water molecules is that the latter lacks a natural acidity, which in the bulk comes about from the presence of hydrated protons in the form of a pH. From known rate data on the autoprotolysis of water, it can be estimated that the average lifetime of a water molecule with respect to the reaction  $\text{H}_2\text{O} \rightarrow \text{H}^+ + \text{OH}^-$  is approximately 13 h. This very slow process is sufficient to maintain a pH of 7 in a beaker of water, but for a cluster containing fewer than 50 water molecules in an experiment lasting  $10^{-4}$  s, it is clearly of no consequence. Therefore, any tendency for a metal ion to promote hydrolysis in a water cluster will take place in the absence of a balancing  $[\text{H}^+]$  concentration, which would normally limit the degree of hydrolysis by bringing the system to equilibrium. No such equilibrium exists in a small cluster, because once formed,  $\text{H}_3\text{O}^+$  or a related ion, for example,  $\text{H}_5\text{O}_2^+$ , is expelled by Coulomb explosion. Figure 7 illustrates this behavior on the part of the  $[\text{Cu}\cdot(\text{H}_2\text{O})_8]^{2+}$  cluster. The mass-selected ion has been excited by collisional activation, which promotes hydrolysis and the loss of  $\text{H}_3\text{O}^+(\text{H}_2\text{O})_n$  for  $n \geq 1$ . In this particular example, there is no evidence for the loss of just  $\text{H}_3\text{O}^+$ . Note that most of the peaks associated with electron transfer are quite broad, which is indicative of a release of kinetic energy resulting from Coulomb repulsion between the two singly charged ions as they separate. In the case of  $[\text{Cu}\cdot(\text{H}_2\text{O})_8]^{2+}$  and most other examples of stable metal ion–water dications, it is necessary to put energy into the ion to promote hydrolysis; but that is obviously not the situation for Sn(II), Hg(II), and Pb(II).

Calculations by Beyer et al.<sup>80</sup> on  $\text{M}^{2+}(\text{H}_2\text{O})_2$  complexes have shown that the activation barrier to proton transfer can be lowered through the formation of a salt bridge. These calculations were particularly successful at accounting for the observation by Spears et al.<sup>23</sup> that  $\text{Ca}^{2+}(\text{H}_2\text{O})_2$  undergoes proton transfer, whereas  $\text{Ca}^{2+}\text{H}_2\text{O}$  is stable. For an arbitrary complex,  $[\text{M}\cdot(\text{H}_2\text{O})_2]^{2+}$ , the relationship between the various ionic species involved in proton transfer has been summarized schematically in Figure 8. In solution, the system would achieve an equilibrium

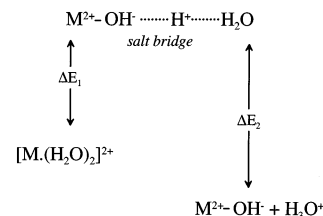
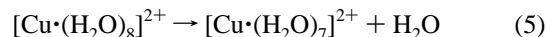


**Figure 8.** Schematic representation of the energetics of the hydrolysis process in isolated cluster ions consisting of a doubly charged metal, M, and several water molecules.  $\Delta E_1$  and  $\Delta E_2$  represent energy barriers to the forward and reverse reactions.

determined by the difference in free energy between the reactants and products and by the ambient pH of the solution. In the gas-phase, reactivity is a one-way process; once beyond the transition state, the products cannot recombine. Thus, what happens in the gas phase will depend solely on the magnitude of  $\Delta E_1$ , which at its most elementary could be equated with the height of the avoided crossing in Figure 1a. As a crude estimate of the internal energy of a complex, it is probably not going to be much larger than the height of the lowest reaction barrier. Thus, in the case of  $[\text{Cu}\cdot(\text{H}_2\text{O})_8]^{2+}$ , the lowest barrier corresponds to the binding energy of a single water molecule. In the absence of any collision gas, the ion exhibits a single unimolecular decay step,



which is promoted through energy remaining in the ion after electron impact ionization, and the intense, narrow peak labeled  $-1$  in Figure 7 is a signature of this reaction. This result would imply that the barrier to electron transfer (ET) is higher in energy than that required to promote reaction 5, hence, the need for collisional activation to observe ET. If we use the binding energy ( $\epsilon_0$ ) as a measure of internal energy, then the above result for  $[\text{Cu}\cdot(\text{H}_2\text{O})_8]^{2+}$  would imply the  $\Delta E_1 > \epsilon_0$ , and a pictorial example of such behavior is shown in the calculations of Beyer et al.<sup>80</sup> An alternative viewpoint would be to argue that  $\Delta E_1$  is increased by solvation (e.g., Figure 1b) because this would then explain the tendency for enhanced levels of electron transfer as the number of water molecules is reduced. Thus, the potential energy surfaces of smaller metallic complexes eventually come close to reproducing the behavior depicted in Figure 8, in which  $\Delta E_1 < \epsilon_0$  and electron-transfer reactions dominate. An example of such behavior is shown in Figure 9 in which the fragmentation pattern of  $[\text{Cu}\cdot(\text{H}_2\text{O})_4]^{2+}$  has been recorded following collisional activation. Features due to the loss of neutral molecules are now very small and electron-transfer products represent a significant fraction of the reaction products. Note that, unlike the result given for  $[\text{Cu}\cdot(\text{H}_2\text{O})_8]^{2+}$ ,  $[\text{Cu}\cdot(\text{H}_2\text{O})_4]^{2+}$  exhibits the loss of  $\text{H}_3\text{O}^+$ .

Relating these ideas to the examples of Sn(II) and Pb(II) (we do not as yet have a satisfactory explanation for the instability of Hg(II) in the presence of water), then we would propose that  $\Delta E_1$  is very small (and in the order Sn(II) < Pb(II)) and that the route to forming a salt bridge is, as a consequence, facile.<sup>81</sup> The arrangement of water molecules in  $[\text{Pb}\cdot(\text{H}_2\text{O})_4]^{2+}$  has already been discussed above (see Figure 5c);<sup>73</sup> the fact that the most stable structure is represented by a primary shell of three molecules, with the additional molecule located in a secondary shell, could be seen as an ideal starting point for the formation of a salt bridge.

Two interesting points arise from the above discussion. First, if a complex is not in a position to form a salt bridge, for

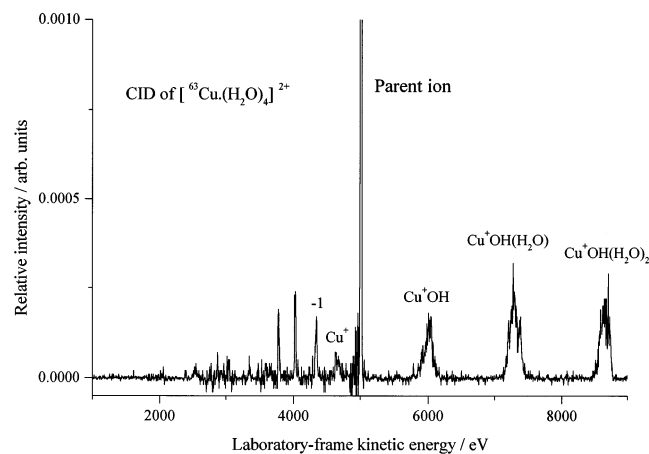


**Figure 9.** Fragmentation pattern recorded for  $[^{63}\text{Cu}\cdot(\text{H}_2\text{O})_4]^{2+}$  following collision-induced dissociation (CID) of the size-selected ion. The parent ion has a laboratory-frame kinetic energy of 5 keV, and fragments are identified according to changes in kinetic energy as a result of dissociation. The narrow peaks denoted as  $-k$  correspond to the loss of  $k$  neutral molecules, and the broad peaks arise from electron-transfer processes for which individual charged fragments are labeled separately.

example, in the  $\text{Mg}^{2+}(\text{H}_2\text{O})\text{Ar}_n$  complexes observed by Velegrakis et al.<sup>82</sup> in which there is only one water molecule, will those ions be more stable than those that contain two or more molecules? The experiments of Shvartsburg and Siu point to many examples in which metal dications are stable in the presence of just a single water molecule.<sup>60</sup> Similarly, the experiments on  $\text{Ca}^{2+}(\text{H}_2\text{O})_2$  suggest there may be other examples in which the presence of two molecules is required to promote the hydrolysis reaction.<sup>23</sup> Second, it is possible to speculate that, above some critical size, two singly charged entities  $\text{MOH}^+$  and  $\text{H}_3\text{O}^+$  might coexist within the same cluster. Experiments on the stability of multiply charged water clusters show that the minimum size of cluster that can accommodate two positive charges is  $(\text{H}_2\text{O})_{36}^{2+}$ ,<sup>83</sup> which has been proposed to have the composition  $(\text{H}_2\text{O})_{35} + \text{H}^+ + \text{OH}^+$ .<sup>84</sup> Thus, a cluster of 35 or more water molecules could be capable of accommodating both  $\text{PbOH}^+$  and  $\text{H}^+$  (or  $\text{H}_3\text{O}^+$ ) without undergoing Coulomb explosion. Recognition and analysis of such a species could have interesting implications for the future study of hydrolysis in the gas phase.

### Observations of the Behavior of $\text{M}^{2+}$ and $\text{M}^{3+}$ Ions with Aprotic Solvents and Ligands

In the absence of any interactions, such as hydrogen bonds, that may lead to an extended molecular network, most aprotic solvents in association with  $\text{M}^{2+}$  ions generate stable structures containing between four and six molecules. Although detailed calculations do not exist, it is probably reasonable to assume that these molecules are all coordinated to the metal ion and that their geometries will be tetrahedral (four molecules) and octahedral (six molecules) whenever ligand repulsion is the only influencing factor. If, for example, ligand field interactions need to be taken into consideration, then other geometries might be anticipated.<sup>13</sup> At this stage in the study of gas-phase complexes, there are no experimental techniques that will provide reliable information on geometry. In the short-term, calculations are the most likely source of structural data.

There have been few experiments performed on triply charged cations,<sup>63,64</sup> and only for one such ion,  $\text{Ho}(\text{III})$ ,<sup>64</sup> have measurements been made on the relative intensities of several complexes

as a function of size. For ligands such as acetone and acetonitrile, intensity maxima were seen at  $n = 6$ , an observation which could equate with the large ionic radius of  $\text{Ho}(\text{III})$  compared with, for example,  $\text{Mg}(\text{II})$ . When similar experiments were undertaken with  $\text{Ho}(\text{III})$  in association with hydrogen-bonded solvents, no ions of the form  $[\text{Ho}(\text{ROH})_n]^{3+}$  ( $\text{R} = \text{H}$  or  $\text{CH}_3$ ) were observed, but instead products of the form  $[\text{HoOR}(\text{ROH})_n]^{2+}$  were detected, which were taken as evidence of the hydrolysis process having occurred as a result of complex formation. Similar observations were recorded by Blades et al. for other members of the lanthanide series.<sup>63</sup> In reference to Table 6, it can be seen that such behavior is consistent with the magnitude of  $pK_{\text{h}}$  for  $\text{Ho}(\text{III})$ .

From experiments on the identification of stable metal–ligand combinations, it is possible to obtain a semiquantitative assessment of what makes a good ligand in terms of its ability to stabilize a metal cation. Two studies of this nature have been undertaken,<sup>30,43</sup> both utilizing a simple model that takes into account the various interactions that might exist between a doubly charged cation and a ligand and between their electron-transfer products. The important terms in those interactions for the combination of a metal ion with a single ligand are

$$E(\text{M}^{2+}-\text{L}) = \Delta - 6.0\mu/r^2 - 28.8\alpha/r^4 \quad (6)$$

and

$$E(\text{M}^+-\text{L}^+) = 14.4/r - 3.0\mu/r^2 - 14.4\alpha/r^4 \quad (7)$$

Where  $\Delta$  is the difference in ionization energy between  $\text{M}^+$  and  $\text{L}$ ,  $\mu$  is taken to be a point dipole for  $\text{L}$ ,  $\alpha$  is the isotropic polarizability of  $\text{L}$ , and  $r$  is the scalar distance between  $\text{M}$  and  $\text{L}$ . The leading term in eq 7 is the Coulomb repulsion between the two separating charges. The units are chosen to give  $E$  in electronvolts. Schematically, the two potential energy curves represented by eqs 6 and 7 are similar to those given in Figure 1a but with the reactive component absent and with the inner repulsive wall of the bound state replaced by a hard-wall potential. The important quantity derived from these relationships is the point at which the two curves cross, because this is a measure of the ease with which the  $\text{M}^{2+}-\text{L}$  moiety will undergo electron transfer. The closer the crossing point is to the equilibrium bond distance, the greater the probability is of electron transfer.

From this analysis, it has been possible to identify the terms in the above equations that contribute to the success of a particular type of ligand (these are shown in bold in Table 4). From the properties listed in Table 4, it can be seen that ionization energy, dipole moment, and polarizability all influence the location of the crossing point. For ligands such as  $\text{CO}_2$ ,  $\text{CH}_3\text{CN}$ , and water in association with magnesium, the calculations reveal that ionization energy is the single most important factor in stabilizing a complex. In the case of  $\text{CO}_2$ , a high ionization energy is paramount in determining the stability of a wide range of  $\text{M}^{2+}-\text{CO}_2$  complexes, particularly in the case of gold(II), for which stable dication complexes are very rare. In a second set of ligands typified, for example, by pyridine, polarizability is the important factor in determining stability. Finally, in a third class of ligand, stability is determined by a combination of dipole moment and polarizability. For two dications,  $\text{Ag}(\text{II})$  and  $\text{Au}(\text{II})$ , it could be shown that an entire group of potential ligands,<sup>30</sup> mainly alcohols, were not capable of stabilizing either ion because of the ease with which electron transfer could occur. Such behavior equates well with the

difficulties encountered in preparing stable Ag(II) and Au(II) complexes in the bulk phase.<sup>13</sup>

### Multiply Charged Anions

There is beginning to emerge a serious experimental program devoted to the study of metallic dianions.<sup>85–88</sup> Ions such as  $\text{CuCl}_4^{2-}$  are clearly representative of the type of complex being considered here, in that the formal oxidation state of the metal ion is +2; however, the distinction between these species and the complexes discussed earlier is that anions rather than neutral molecules now surround the central ion. The net effect in the case of  $\text{CN}^-$ ,  $\text{Cl}^-$ , and  $\text{Br}^-$  is to give the species an overall doubly negative charge. Several groups have begun using electrospray to generate ions of the type  $\text{Pt}(\text{CN})_6^{2-}$ ,  $\text{PtCl}_4^{2-}$ ,  $\text{PtBr}_4^{2-}$ , etc.<sup>85–88</sup> and in the case of Wang et al.<sup>85,86</sup> to also study their photoelectron spectra. Because a recent gas-phase study has provided evidence of  $\text{Pt}(\text{CN})_6^{2-}$ ,  $\text{Pt}(\text{CN})_5^{2-}$ , and  $\text{Pt}(\text{CN})_4^{2-}$ ,<sup>87</sup> it is clear that these experiments could provide access to a wide range of transition metal oxidation states.

A particularly interesting concept, which has been identified from these experiments, is that of a repulsive Coulomb barrier (RCB).<sup>89</sup> In contrast to the repulsive Coulomb interactions encountered thus far, a RCB arises from the displacement of electrons away from the charged core of an anion. For most stable dianions, the electrons are held in place by a valence potential that operates over short distances. If one electron is displaced, it begins to experience a repulsive Coulomb interaction of magnitude  $e^2/R$  with the remaining valence electron, and if  $R$  is sufficiently large, the repulsive contribution dominates behavior. The experimental implication of such a barrier is that electron photodetachment experiments are required to use photons with an energy close to the value of the RCB.<sup>85,86</sup> Thus, it is necessary to measure the kinetic energies of ejected electrons to extract adiabatic binding energies. Electrons have also been shown to tunnel through the RCB.<sup>88</sup>

### Directions for the Future

**(i) Binding Energies.** Very few of the studies discussed thus far have led to an experimental measurement of the binding energy between a metal dication and a ligand. In contrast, there is a large number of theoretical papers devoted to this topic. As noted by Kebarle and co-workers,<sup>34</sup> the high binding energies of ligands in small  $[\text{M}\cdot\text{L}_n]^{2+}$  complexes mean that they are not thermally labile at the temperatures typically used in experiments in which equilibrium properties ( $\Delta G^0$ ,  $\Delta H^0$ , and  $\Delta S^0$ ) are measured. Therefore, techniques that rely on maintaining an equilibrium once ions have been prepared, for example, by electrospray, are only effective for binding enthalpies that are  $\leq 30 \text{ kJ mol}^{-1}$ . Thus, in the case of  $[\text{Mg}\cdot(\text{H}_2\text{O})_n]^{2+}$  ions, this limitation means that  $n$  has to be  $\geq 5$ .

An alternative approach used by Williams and co-workers examines the decay kinetics of  $[\text{M}\cdot(\text{H}_2\text{O})_n]^{2+}$  ions trapped at low pressures in an FTICR instrument.<sup>35–37</sup> Experimental data has so far been presented for  $\text{Ni}^{2+}$  and a series of alkaline earth metal dications. Arrhenius parameters derived from the kinetic data include an activation energy, which because the reverse barrier for water attachment is negligible can be equated with the binding enthalpy. However, the size of complex that can be treated in this manner is again limited to  $n \geq 5$ . There is reasonably good agreement between the kinetic results of Williams and co-workers and the van't Hoff equilibrium measurements of Kebarle and co-workers; however, the data set accessible from the latter experiments is far more extensive.

An unexpected result to emerge from the experiments on trapped ions is evidence of two isomers for the ion  $[\text{Mg}\cdot(\text{H}_2\text{O})_6]^{2+}$ :<sup>36</sup> a low-temperature version in which all six molecules are thought to be located in the primary solvation shell and a high-temperature variant in which two molecules are promoted to an outer shell. The structure of the latter ion is thought to be very similar to that presented for  $[\text{Mn}\cdot(\text{H}_2\text{O})_6]^{2+}$  in Figure 5. Further evidence of isomers in smaller  $[\text{Mg}\cdot(\text{H}_2\text{O})_n]^{2+}$  complexes has come from recent experiments involving collision-induced fragmentation.<sup>51</sup>

A possible route to obtaining binding energies for smaller multiply charged complexes is through the technique developed by Armentrout and co-workers,<sup>90</sup> whereby ions are injected into a collision gas at ever decreasing kinetic energies until a fragment ion appearance threshold is reached. By modeling the collision cross-section as a function of relative kinetic energy and internal energy state populations, accurate bond dissociation energies can be obtained. Thus far, application of the technique has been restricted to singly charged ions; however, it may prove to be one of the few methods available for overcoming the very large ( $350 \text{ kJ mol}^{-1}$ ) binding energies predicted for small  $\text{Mg}^{2+}/\text{Ca}^{2+}$ -water complexes.<sup>34</sup>

**(ii) Spectroscopy.** The spectroscopy of multiply charged metal-ligand complexes is possibly one of the most significant topics to be addressed; however, it could also prove to be one of the most difficult areas to investigate in terms of the available experimental techniques. Of the current methods available for generating  $[\text{M}\cdot\text{L}_n]^{2+}$  complexes (electrospray and pick-up), neither is likely to ever yield ion signals greater than  $10^{-12}$ – $10^{-10}$  A. Such signals are far too low for any form of direct absorption spectroscopy, although for electronic transitions it may be possible to measure fluorescence excitation spectra on trapped ions provided that they do not undergo collisional relaxation (radiative lifetimes associated with forbidden transitions may be much longer than the average time between collisions under the conditions at which the average trap operates). Given these considerations, the most effective ways of accessing spectroscopic transitions are probably via either photofragmentation or through monitoring signal depletion; these techniques having proved to be remarkably successful in the study of singly charged metal-ligand complexes over a wide range of wavelengths.<sup>91</sup>

There are some important differences between the spectroscopy of singly and doubly charged complexes, particularly where transition metals are concerned. The spectroscopy of the latter is more likely to cover a broader range of the visible spectrum than is seen, for example, in singly charged alkaline earth complexes.<sup>91</sup> However, whereas almost all transitions in ions such as  $\text{Mg}^+$  and  $\text{Sr}^+$  are allowed ( $^2\text{P} \leftarrow ^2\text{S}$ ), those involving transition metal ions fall broadly into two categories: (i) charge transfer and, therefore, strongly allowed; (ii) ligand field in the form of d-d transitions, which are Laporte forbidden (because  $\Delta l = 0$ ) and (sometimes) spin-forbidden.<sup>13</sup> Although there is some relaxation of the parity selection rule in complexes without inversion centers, in general it can be expected that extinction coefficients associated with ligand field transitions will be 3 or 4 orders of magnitude lower than those typical of many ions previously studied in the gas phase. Compounded with the low ion signals, it is apparent that studies in the gas phase of ligand field transitions involving metal ions in their more common oxidation states represent a very considerable challenge.

Having said that, some significant advances have been made recently using both photofragmentation and signal depletion to record electronic spectra from transition metal complexes. Posey

and co-workers were the first to present spectra that were recorded from the low-spin iron(II) complexes  $[\text{Fe} \cdot (\text{bpy})_3]^{2+}$  and  $[\text{Fe} \cdot (\text{terpy})_2]^{2+}$ ,<sup>38,39</sup> both of which exhibit a metal–ligand charge (electron) transfer (MLCT) transition at visible wavelengths. By utilizing electrospray to solvate the ions, they were able to study the evolution of spectral features as a function of the numbers of solvent molecules. Preliminary results from a study of ligand–metal charge (electron) transfer (LMCT) in the complexes  $[\text{Cu} \cdot (\text{pyridine})_n]^{2+}$  and  $[\text{Ag} \cdot (\text{pyridine})_n]^{2+}$  were recently presented by Puskar et al.<sup>54</sup> Examples of the observed fragmentation patterns were presented earlier (Figure 4) as part of a discussion on the consequence of excitation/fragmentation on the part of doubly charged complexes. Both of these studies benefited from the high extinction coefficients of charge-transfer transitions.

Several examples of ligand field d–d transitions recorded in the gas phase have also been presented recently. Metz and co-workers have studied the systems  $[\text{Co} \cdot (\text{H}_2\text{O})_n]^{2+}$  and  $[\text{Ni} \cdot (\text{H}_2\text{O})_n]^{2+}$  using a combination of electrospray, ion trap, and time-of-flight mass spectrometry.<sup>40,41</sup> Signal integration within the trap is one way of overcoming the problem of low ion number density. As a function of laser wavelength, the photo-fragmentation patterns of both  $[\text{Co} \cdot (\text{H}_2\text{O})_4]^{2+}$  and  $[\text{Co} \cdot (\text{H}_2\text{O})_6]^{2+}$  exhibited features very similar to those seen in the aqueous phase. Likewise, a study of the ion  $[\text{Cu} \cdot (\text{pyridine})_4]^{2+}$  at visible wavelengths yielded an extinction coefficient and wavelength dependence comparable to those measured for Cu(II) complexes in the condensed phase.<sup>55</sup> A similar study of  $[\text{Ag} \cdot (\text{pyridine})_4]^{2+}$  called into question the interpretation of the condensed-phase data,<sup>55</sup> the gas-phase results showing strong evidence of a ligand–d charge-transfer transition rather than a d–d transition.

The prospect of being able to study the electronic spectra of multiply charged anions, such as  $\text{CuCl}_4^{2-}$ , offers an interesting challenge, which could yield some very exciting results.  $\text{CuCl}_4^{2-}$  in particular has a comparatively simple geometry and electronic structure, and there exist some excellent examples of spectra recorded in the condensed phase.<sup>92,93</sup>

**(iii) Model Bioinorganic Systems.** Few gas-phase studies have thus far explored the potential for modeling bioinorganic systems.<sup>42</sup> However, the ability to construct an environment for a metal ion, such as  $\text{Zn}^{2+}$ , that mimics the constrained conditions of dielectric saturation that probably exist in a biological active site<sup>12</sup> offers many new opportunities. Likewise, it may be possible to synthesize model blue copper sites which, because they are in the gas phase, can resist the tendency for the central Cu(II) ion to be reduced to Cu(I).<sup>12,25</sup> Several recent experiments have demonstrated that oxidation states that are unstable in the bulk can be prepared and studied in the gas phase.<sup>30,45</sup>

## Conclusion

The most obvious question to arise from this discussion is “how close are we with multiply charged ions to reproducing behavior in the bulk?” For elementary qualitative properties, such as ligand configuration, then it is evident that the core cationic units of many solid-state complexes can be constructed in the gas phase. There exist so few examples of spectroscopy that it is difficult to attribute particular features as being the consequences of an emerging solvent structure. If we revert to our original criterion of bulk solvation, as exemplified by Table 2, then it is possible to use calculated incremental ligand binding energies to estimate the contribution to hydration enthalpy from a primary shell of water molecules. This has been done in Figure 10, in which data have been taken from ref 94 and compared with the bulk hydration enthalpies given in Table 6. As can be

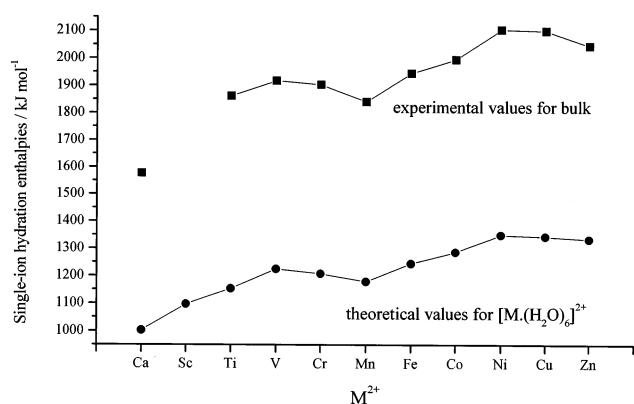


**Figure 10.** Comparison between experimental single-ion hydration enthalpies and theoretical results calculated for  $[\text{M} \cdot (\text{H}_2\text{O})_6]^{2+}$ . The latter data have been taken from ref 94. There are no experimental data for  $\text{Sc}^{2+}$ .

seen, the binding energies of the first six water molecules constitute approximately 60% of the bulk hydration enthalpy.<sup>94</sup> There are minor corrections to be made to the calculated data, along the lines of those discussed for single charge ions;<sup>11</sup> however, it is obvious that the influence of a 2+ charge on the metal ion extends well beyond the first solvation shell. Some of the structures discussed in the text confirm this conclusion in that the formation of charge-enhanced hydrogen bonds make a significant contribution to the development of secondary solvation shells, frequently at the expense of primary coordination to the central metal ion. A more thorough comparison between gas-phase and bulk data has been provided by the results of Peschke et al.,<sup>34</sup> who have combined theory and experiment to yield gas-phase hydration enthalpies for  $\text{Mg}^{2+}$  and  $\text{Ca}^{2+}$  surrounded by up to 14 water molecules. The results are as follows:  $\text{Mg}^{2+}$  –1826.6 kJ mol<sup>-1</sup> (gp), –1998 kJ mol<sup>-1</sup> (bulk);  $\text{Ca}^{2+}$  –1487 kJ mol<sup>-1</sup> (gp), –1669 kJ mol<sup>-1</sup> (bulk). As can be seen, there is still a shortfall of ~160 kJ mol<sup>-1</sup> even with contributions from a significant second solvation shell. As noted by Peschke et al.,<sup>34</sup> the gas-phase data are close to reproducing the difference  $\Delta H_h(\text{Mg}^{2+}) - \Delta H_h(\text{Ca}^{2+})$ , which in the bulk is ~330 kJ mol<sup>-1</sup> compared with ~340 kJ mol<sup>-1</sup> (gp).

As noted earlier, it would appear that there is more of an implicit relationship between a doubly charged ion and a solvent than is true of singly charged ions under similar conditions. The experimental results discussed above would suggest that the contributions made by individual molecules to many of the physical properties associated with doubly and triply charged ions in the condensed phase extend well into the second coordination shell. Therefore, an accurate gas-phase picture of such processes as solvation may require detailed knowledge of the coordination of some 20–30 separate molecules. The past 5 years has seen significant advances in the study of multiply charged metal ion complexes in the gas phase, the most important being the development of techniques for generating a wide range of stable  $[\text{M} \cdot \text{L}_m]^{n+}$  species, with the success of both electrospray and the pick-up method offering new opportunities for exploring metal ions in their more common oxidation states.

**Acknowledgment.** The author thanks B. Duncombe and Dr. L. Puskar for their careful reading of the manuscript. Acknowledgment is also made of the valuable contributions from Dr. C. A. Woodward, Dr. M. P. Dobson, Dr. P. E. Barran, Dr. N. R. Walker, Dr. R. R. Wright, Dr. H. Cox, and G. Akibo-Betts to the success of the work discussed here. The author would also like to thank EPSRC for their continued financial support.

## References and Notes

- (1) *Physics and Chemistry of Small Clusters*; Jena, P., Rao, B. K., Khanna, S. N., Eds.; Nato ASI Series, Vol. 158; Plenum Press: New York, 1986.
- (2) Buffat, Ph.; Borel, J.-P. *Phys. Rev.* **1976**, *A13*, 2287.
- (3) Rademann, K.; Kaiser, B.; Even, U.; Hensel, F. *Phys. Rev. Lett.* **1987**, *59*, 2319.
- (4) Echt, O.; Sattler, K.; Recknagel, E. *Phys. Rev. Lett.* **1981**, *47*, 1121.
- (5) Farges, J.; de Feraudy, M. F.; Raoult, B.; Torchet, G. In *Physics and Chemistry of Small Clusters*; Jena, P., Rao, B. K., Khanna, S. N., Eds.; Nato ASI Series, Vol. 158; Plenum Press: New York, 1986; p 15.
- (6) Kebarle, P. *Annu. Rev. Phys. Chem.* **1977**, *74*, 1466.
- (7) Keesee, R. G.; Castleman, A. W., Jr. *J. Phys. Chem. Ref. Data* **1986**, *15*, 1011.
- (8) Adapted from data given in ref 6.
- (9) Smith, D. W. *J. Chem. Educ.* **1977**, *54*, 540.
- (10) Markovich, G.; Pollack, S.; Giniger, R.; Cheshnovsky, O. *J. Chem. Phys.* **1994**, *101*, 9344.
- (11) Coe, J. V. *Chem. Phys. Lett.* **1994**, *229*, 161.
- (12) Frausto da Silva, J. J. R.; Williams, R. J. P. *The Biological Chemistry of the Elements*; Clarendon Press: Oxford, U.K., 1997.
- (13) Cotton, F. A.; Wilkinson, G. *Advanced Inorganic Chemistry*; Wiley: London, 1988.
- (14) Misaizu, F.; Sanekata, M.; Tsukamoto, K.; Fuke, K.; Iwata, S. *J. Phys. Chem.* **1992**, *96*, 8259.
- (15) Harms, A. C.; Khanna, S. N.; Chen, B.; Castleman, A. W., Jr. *J. Chem. Phys.* **1994**, *100*, 3540.
- (16) Weast, R. C. *Handbook of Chemistry and Physics*; CRC Press: Boca Raton FL, 1985.
- (17) Tokyn, R.; Weisshaar, J. C. *J. Am. Chem. Soc.* **1986**, *108*, 7128.
- (18) Echt, O.; Mark, T. D. In *Clusters of Atoms and Molecules II*; Haberland, H., Ed.; Springer-Verlag: Berlin, 1994; p 183.
- (19) Gill, P. M. W.; Radom, L. *Chem. Phys. Lett.* **1987**, *136*, 294.
- (20) Schroder, D.; Schwarz, H. *J. Phys. Chem. A* **1999**, *103*, 7385.
- (21) El-Nahas, A. M. *Chem. Phys. Lett.* **2001**, *345*, 325.
- (22) Walker, N. R.; Wright, R. R.; Barran, P. E.; Cox, H.; Stace, A. J. *J. Chem. Phys.* **2001**, *114*, 5562.
- (23) Spears, K. G.; Fehsenfeld, F. C.; McFarland, M.; Ferguson, E. E. *J. Chem. Phys.* **1972**, *56*, 2562.
- (24) Marcus, R. A. *Annu. Rev. Phys. Chem.* **1964**, *15*, 155.
- (25) Frausto da Silva, J. J. R.; Williams, R. J. P. *The Biological Chemistry of the Elements*; Clarendon Press: Oxford, U.K., 1997; p 389.
- (26) Lippard, S. J.; Berg, J. M. *Principles of Bioinorganic Chemistry*; University Science Books: Mill Valley, CA, 1994; p 27.
- (27) Dainton, F. S.; James, D. G. L. *Trans. Faraday Soc.* **1958**, *54*, 649.
- (28) Stace, A. J.; Walker, N. R.; Firth, S. *J. Am. Chem. Soc.* **1997**, *119*, 10239.
- (29) Wright, R. R.; Walker, N. R.; Firth, S.; Stace, A. J. *J. Phys. Chem. A* **2001**, *105*, 54.
- (30) Walker, N. R.; Wright, R. R.; Stace, A. J. *J. Am. Chem. Soc.* **1999**, *121*, 4837.
- (31) Walker, N. R.; Wright, R. R.; Barran, P. E.; Murrell, J. N.; Stace, A. J. *J. Am. Chem. Soc.* **2001**, *123*, 4223.
- (32) Blades, A. T.; Jayaweera, P.; Ikononou, M. G.; Kebarle, P. *Int. J. Mass Spectrom. Ion Processes* **1990**, *102*, 251.
- (33) Blades, A. T.; Jayaweera, P.; Ikononou, M. G.; Kebarle, P. *J. Chem. Phys.* **1990**, *92*, 5900.
- (34) Cheng, Z. L.; Siu, K. M.; Guevremont, R.; Berman, S. S. *J. Am. Soc. Mass Spectrom.* **1992**, *3*, 281.
- (35) Peschke, M.; Blades, A. T.; Kebarle, P. *J. Phys. Chem. A* **1998**, *102*, 9978.
- (36) Rodriguez-Cruz, S. E.; Jockusch, R. A.; Williams, E. R. *J. Am. Chem. Soc.* **1998**, *120*, 5842.
- (37) Rodriguez-Cruz, S. E.; Jockusch, R. A.; Williams, E. R. *J. Am. Chem. Soc.* **1999**, *121*, 1986.
- (38) Rodriguez-Cruz, S. E.; Jockusch, R. A.; Williams, E. R. *J. Am. Chem. Soc.* **1999**, *121*, 8898.
- (39) Spence, T. G.; Burns, T. D.; Guckenberger, G. B.; Posey, L. A. *J. Phys. Chem. A* **1997**, *101*, 1081.
- (40) Spence, T. G.; Trotter, B. T.; Posey, L. A. *J. Phys. Chem. A* **1998**, *102*, 7779.
- (41) Thompson, C. J.; Husband, J.; Aguirre, F.; Metz, R. B. *J. Phys. Chem. A* **2000**, *104*, 8155.
- (42) Faherty, K. P.; Thompson, C. J.; Aguirre, F.; Michne, J.; Metz, R. B. *J. Phys. Chem. A* **2001**, *105*, 10054.
- (43) Peschke, M.; Blades, A. T.; Kebarle, P. *J. Am. Chem. Soc.* **2000**, *122*, 1492.
- (44) Walker, N.; Dobson, M. P.; Wright, R. R.; Barran, P. E.; Murrell, J. N.; Stace, A. J. *J. Am. Chem. Soc.* **2000**, *122*, 11138.
- (45) Wright, R. R.; Walker, N. R.; Firth, S.; Stace, A. J. *J. Phys. Chem. A* **2001**, *105*, 54.
- (46) Walker, N. R.; Wright, R. R.; Barran, P. E.; Stace, A. J. *Organometallics* **1999**, *18*, 3569.
- (47) Dobson, M. P.; Stace, A. J. *J. Chem. Soc., Chem. Commun.* **1996**, 1553.
- (48) Duncombe, B.; Cox, H.; Stace, A. J. Unpublished results.
- (49) Akibo-Betts, G.; Barran, P. E.; Stace, A. J. *Chem. Phys. Lett.* **2000**, *329*, 431.
- (50) Cox, H.; Akibo-Betts, G.; Wright, R. R.; Walker, N. R.; Curtis, S.; Duncombe, B.; Stace, A. J., submitted for publication.
- (51) Puskar, L.; Stace, A. J. Unpublished results.
- (52) Barran, P. E.; Walker, N. R.; Stace, A. J. *J. Chem. Phys.* **2000**, *112*, 6173.
- (53) Dobson, M. P.; Stace, A. J. *Int. J. Mass Spectrom. Ion Processes* **1997**, *165/166*, 5.
- (54) Walker, N. R.; Firth, S.; Stace, A. J. *Chem. Phys. Lett.* **1998**, *292*, 125.
- (55) Puskar, L.; Barran, P. E.; Wright, R. R.; Kirkwood, D. A.; Stace, A. J. *J. Chem. Phys.* **2000**, *112*, 7751.
- (56) Puskar, L.; Stace, A. J. *J. Chem. Phys.* **2001**, *114*, 6499.
- (57) El-Nahas, A. M.; Tajima, N.; Hirao, K. *Chem. Phys. Lett.* **2000**, *318*, 333.
- (58) Stace, A. J.; Walker, N. R.; Wright, R. R.; Firth, S. *Chem. Phys. Lett.* **2000**, *329*, 173.
- (59) Schroder, D.; Schwarz, H.; Jianglin, W.; Wesdemiotis, C. *Chem. Phys. Lett.* **2001**, *343*, 258.
- (60) Stone, J. A.; Vukomanovic, D. *Chem. Phys. Lett.* **2001**, *346*, 419.
- (61) Shvartsburg, A. A.; Siu, K. W. M. *J. Am. Chem. Soc.* **2001**, *123*, 10071.
- (62) Akibo-Bett, G.; Barran, P. E.; Puskar, L.; Duncombe, B.; Cox, H.; Stace, A. J., submitted for publication.
- (63) Stone, J. A. Private communication.
- (64) Blades, A. T.; Jayaweera, P.; Ikononou, M. G.; Kebarle, P. *Int. J. Mass Spectrom. Ion Processes* **1990**, *101*, 325.
- (65) Walker, N. R.; Stace, A. J.; Woodward, C. A. *Int. J. Mass Spectrom. Ion Processes* **1999**, *179/180*, 253.
- (66) Stace, A. J.; Moore, C. *Chem. Phys. Lett.* **1983**, *96*, 80.
- (67) Lethbridge, P. G.; Stace, A. J. *J. Chem. Phys.* **1988**, *89*, 4062.
- (68) Mark, T. D.; Scheier, P. *Chem. Phys. Lett.* **1987**, *137*, 245.
- (69) Stone, J. A.; Vukomanovic, D. *Int. J. Mass Spectrom. Ion Processes* **1999**, *185-187*, 227.
- (70) Shvartsburg, A. A. Private communication.
- (71) Stace, A. J. *Phys. Chem. Chem. Phys.* **2001**, *3*, 1935.
- (72) Bércecs, A.; Nukada, T.; Margl, P.; Ziegler, T. *J. Phys. Chem. A* **1999**, *103*, 9693.
- (73) Pavlov, M.; Siegbahn, P. E. M.; Sandström, M. *J. Phys. Chem. A* **1998**, *102*, 219.
- (74) Akibo-Betts, G.; Barran, P. E.; Puskar, L.; Duncombe, B.; Cox, H.; Stace, A. J. *J. Am. Chem. Soc.*, in press.
- (75) Ohtaki, H.; Radnai, T. *Chem. Rev.* **1993**, *93*, 1157.
- (76) Baes, C. F., Jr.; Mesmer, R. E. *The Hydrolysis of Cations*; Wiley: New York, 1976.
- (77) Pearson, R. G. *J. Chem. Educ.* **1963**, *45*, 581 and 646.
- (78) Adapted from Shriver, D. F.; Atkins, P. W. *Inorganic Chemistry*; Oxford University Press: Oxford, U.K., 1999.
- (79) Conway, B. E. *Ionic Hydration in Chemistry and Biophysics*; Elsevier: Amsterdam, 1981.
- (80) Huheey, J. E.; Keiter, E. A.; Keiter, R. L. *Inorganic Chemistry*; Harper Collins: New York, 1993.
- (81) Beyer, M.; Williams, E. R.; Bondybey, V. E. *J. Am. Chem. Soc.* **1999**, *121*, 1565.
- (82) Cox, H.; Stace, A. J., manuscript in preparation.
- (83) Velegrakis, M.; Lüder, C. *Chem. Phys. Lett.* **1994**, *223*, 139.
- (84) Stace, A. J. *Phys. Rev. Lett.* **1988**, *61*, 306.
- (85) Stace, A. J. *Chem. Phys. Lett.* **1990**, *174*, 103.
- (86) Wang, X.-B.; Ding, C.-F.; Wang, L.-S., *Phys. Rev. Lett.* **1998**, *81*, 3351.
- (87) Wang, X.-B.; Wang, L.-S. *Nature (London)* **1999**, *400*, 245.
- (88) Bojesen, G.; Hvelplund, P.; Jørgensen, T. J. D.; Nielsen, S. B. *J. Chem. Phys.* **2000**, *113*, 6608.
- (89) Blom, M. N.; Hampe, O.; Gilb, S.; Weis, P.; Kappes, M. M. *J. Chem. Phys.* **2001**, *115*, 3690.
- (90) Simons, J.; Skurski, P.; Barrios, R. *J. Am. Chem. Soc.* **2000**, *122*, 11893.
- (91) Ervin, K. M.; Armentrout, P. B. *J. Chem. Phys.* **1985**, *83*, 166.
- (92) Duncan, M. A. *Annu. Rev. Phys. Chem.* **1997**, *48*, 69.
- (93) Hitchman, M. A.; Cassidy, P. J. *Inorg. Chem.* **1979**, *18*, 1745.
- (94) Desjardins, S. R.; Penfield, K. W.; Cohen, S. L.; Musselman, R. L.; Solomon, E. I. *J. Am. Chem. Soc.* **1983**, *105*, 4590.
- (95) Åkesson, R.; Pettersson, L. G. M.; Sandström, M.; Wahlgren, U. *J. Am. Chem. Soc.* **1994**, *116*, 8691.